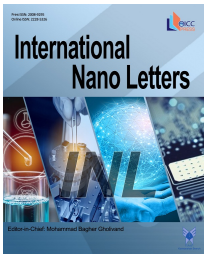

Volume 15, Issue 2, 152507 (1-4)

International Nano Letters (INL)

https://doi.org/10.57647/inl.2025.1502.07

Tailoring Electronic and Magnetic Behaviour of ZnS via (Sm, Co) Co-Doping for Spintronics Applications

D. Saikia[1,*], J. P. Borah[2]

[1]*Department of Physics, Duliajan College, Dibrugarh, Duliajan-786602, Assam, India.*
[2]*National Institute of Technology Nagaland, Dimapur, Nagaland 787103, India.*

[*]**Corresponding author:** dipraj.saikia7@gmail.com

Original Research

Received:
22 April 2025
Revised:
29 May 2025
Accepted:
15 June 2025
Published in Issue:
30 June 2025

Abstract:

Exploring semiconducting materials for applications in the spintronic devices we investigate structural, electronic and magnetic properties of (Sm, Co) Co-doped ZnS diluted magnetic semiconductor ($Zn_{30}Sm_1Co_1S_{32}$) by first principle calculations using GGA+U approximation. The total energy calculations depict the ferromagnetic state as the stable state in the Co-doped system with larger Sm-Co separation while for smaller Sm-Co separation the system shows antiferromagnetic character. The total density of states (DOS) calculations demonstrates semiconducting and metallic character in the spin up and spin down states respectively which discloses p-d hybridization between Co-d and S-p ion revealing half metallic behaviour with 100% spin polarization. These findings establish $Zn_{30}Sm_1Co_1S_{32}$ as promising material for spintronic applications, combining semiconductor functionality with magnetic ordering and spin polarization essential for next-generation electronic devices

Keywords: Spintronics; Diluted magnetic semiconductors; Half metallic ferromagnetism; p-d Hybridization

Cite this article: Saikia, D., Borah, J.P. Tailoring Electronic and Magnetic Behaviour of ZnS via (Sm, Co) Co-Doping for Spintronics Applications. *Int. Nano Lett.* **15**(2), 152507 (2025).

1. Introduction

Diluted magnetic semiconductors (DMS) have recently been enchanting a significant attention in the field of magnetic semiconductor research due to their remarkable applications in the spintronic devices [1–4]. High spin polarized nature of these materials leading room temperature ferromagnetism (RTFM) is the key paramater in the spin transport devices [5–7]. The 3d transition metal (TM) doped zinc blende structured II-VI semiconductors have become potential DMS candidates due to their higher solubile nature, electronic, optical and magnetic properties compared to those of the III-V or II-V compounds [8, 9]. Extensive attention has been devoted to the Density functional theory (DFT) calculations in order to investigate the electronics structures of DMSs which demonstrates the actual mechanisms that are responsible for RTFM [10, 11]. The half metallic transition metal [Mn, Ni, Fe, Co, Cr etc.] doped II-VI DMSs can be efficiently exploited in the spintronic devices [7, 8, 12]. Besides TM, rare earth (RE) metals (Gd, Sm etc.) can be effectively utilized for developing DMSs as they have higher magnetic moment as compared to the TM ions [13, 14]. Recently Co-doping of rare earth metal with TM ions in II-VI semiconductor has become a vital approach in achieving half metallic behaviour in DMSs [15, 16]. Among various host materials, ZnS has been one of the most promising II-VI semiconductors due to its higher band gap (3.68 eV) and remarkable optical and electronic properties [7, 17]. Taking account to these, we have studied the electronic and magnetic properties of (Sm, Co) Co-doped ZnS diluted magnetic semiconductor by first principle calculations.

2. Computational details

All the spin polarized density functional theory calculations were carried out by QUANTUM ESPRESSO codes [18]. The exchange–correlation energies were described by the spin polarized generalized gradient approximation with Hubbard correction (GGA+U) term (U = 5

eV and 6 eV for 3d and 4f electrons of Co and Sm) by Perdew–Burke–Ernzerhof (PBE) functional [19, 20]. The kinetic energy cut-off is set to 25 Ry. The Brillouin zone was sampled by $4 \times 4 \times 4$ Monkhorst-Pack grid and the unit cell was relaxed using the force convergence threshold of 10^{-3} Ry a.u.$^{-1}$. Broyden–Fletcher–Goldfarb–Shanno (BFGS) algorithm with the cell optimization criterion (force tolerance of 0.06 eV/Å, stress tolerance of 0.01 GPa, and displacement of 0.2 Å) [21] was used for geometry optimization. To study the electronic and magnetic properties of (Sm, Co) Co-doped ZnS, we consider $2 \times 2 \times 2$ supercell of zinc blende replacing two Zn atoms by Sm and Co atoms in two different positions (Fig. 1).

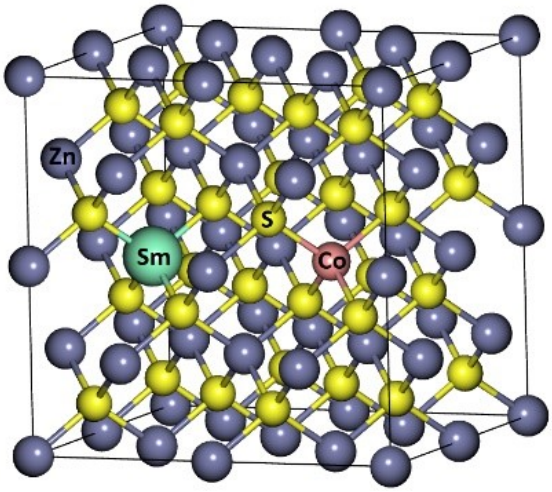

Figure 1. Crystal structure of (Sm, Co) Co-doped ZnS.

3. Results and discussions

In order to optimize the structural parameters for $Zn_{30}Sm_1Co_1S_{32}$ system, we plot total ground state energy with respect to the unit cell volume using Murnaghan's equation of states [22] with SGGA approximation in both ferromagnetic and antiferromagnetic states as shown in the Fig. 2. The calculated values of lattice parameter (a), bulk modulus (B) and the first order derivative of Bulk modulus ($B^{/}$) for $Zn_{30}Sm_1Co_1S_{32}$ with Co-Sm separation of 2.97 Å are found to be 5.47 Å, 63.75 (GPa) and 5.36 respectively. The lattice parameter is found to be increased as compared to bulk ZnS system which is due to the higher ionic radius of Sm^{3+} ion (0.95 Å) than that of Co^{2+} (0.58 Å) and Zn^{2+} (0.74 Å) [23].

In order to find the magnetic stability and magnetic coupling of the $Zn_{30}Sm_1Co_1S_{32}$ system we have calculated total defect formation energy and energy difference (ΔE) between ferromagnetic (FM) and antiferromagnetic (AFM) state replacing two Zn atoms by two Sm and Co atoms for four different Sm-Co separations in the $2 \times 2 \times 2$ periodic supercell (Fig. 3). The calculated values of ΔE for different Sm-Co separations is shown in the Table 1. The negative value of ΔE in the case of smaller Sm-Co separation (2.43 Å) demonstrates that the antiferromagnetic state is energetically more favourable than the ferromagnetic state while the positive values of ΔE for higher Sm-Co separations demonstrates

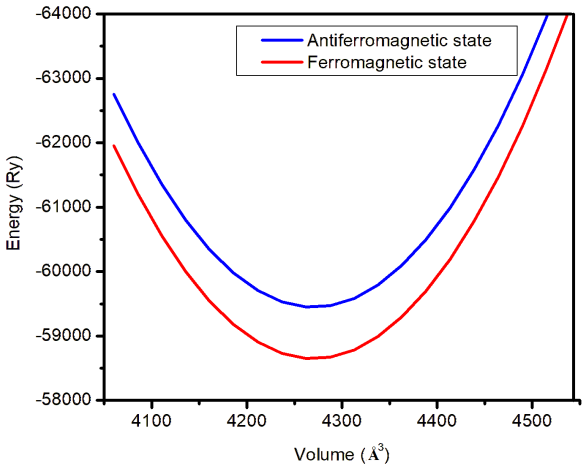

Figure 2. Variation of total energy (Ry) with respect to unit cell volume (Å^3) of $Zn_{30}Sm_1Co_1S_{32}$ for Co-Sm separation of 2.97 Å (configuration II in the Table 1).

the ferromagnetic state as more energetically favourable than the antiferromagnetic state [23]. For smaller Sm-Co separation, the enhanced short range antiferromagnetic interaction dominates over ferromagnetic interaction whereas for higher Sm-Co separation, the long-range ferromagnetic coupling ensues and the system becomes ferromagnetic in nature [24]. Moreover, it is observed from the Table 1 that the variation of ΔE with Sm-Co separation shows an oscillatory magnetic order with increasing Sm-Co separation demonstrating indirect Ruderman–Kittel–Kasuya–Yosida (RKKY) interactions which was observed in our previous study [24]. Negative values of formation energies obtained in all the configurations, depicts that Sm, Co co-doped ZnS system can be easily fabricated experimentally [24, 25].

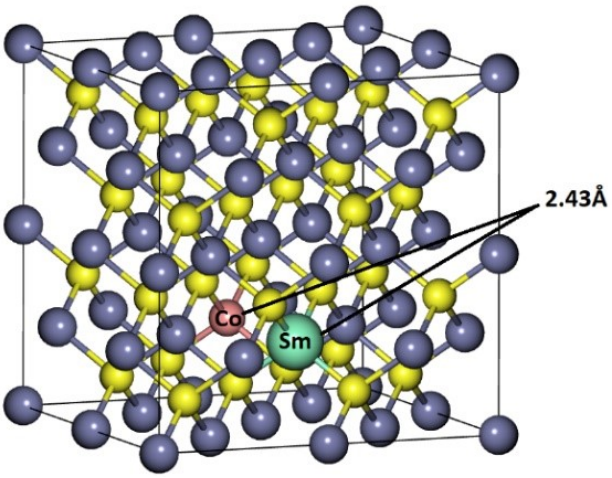

Figure 3. Sm, Co Co-doped ZnS for Sm-Co separation of 2.43 Å.

Electronic properties

The spin polarized density of states (DOS) of $Zn_{30}Sm_1Co_1S_{32}$ system with Co-Sm separation of 2.97 Å as calculated by GGA+U approximation is depicted in Fig. 4 (a). The fermi level (EF) is represented by the vertical solid line with zero energy. The postitive

Table 1. Formation energy and energy difference between AFM and FM states of $Zn_{30}Sm_1Co_1S_{32}$.

Configuration	Sm-Co separation (Å)	EFM (eV)	EAFM (eV)	Energy difference (ΔE) (meV)	Formation energy (eV)
I	2.43	−56,864.5795	−56,864.6416	−62.1	−1.02
II	2.97	−51,725.6742	−51,725.6277	46.5	−0.98
III	3.26	−46,463.2709	−46,463.2146	56.3	−0.76
IV	4.06	−42,643.8153	−42,643.7827	32.6	−0.64

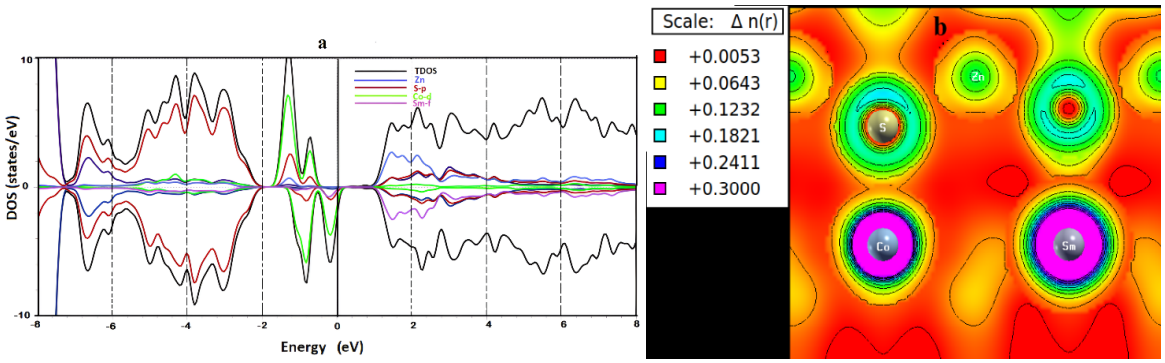

Figure 4. (a) Spin polarized Density of States (DOS) of $Zn_{30}Sm_1Co_1S_{32}$ (b) Charge density plot of $Zn_{30}Sm_1Co_1S_{32}$.

and negative values of DOS represent the spin up and spin down states respectiviely. The black line represents the total DOS, blue, brown, green and purple lines represent Zn-s, S-3p, Co-3d and Sm-4f states. The total DOS shows semiconducting nature in the spin up state with a band gap of 1.42 eV and metallic character in the spin down state indicating half metallic character with 100% spin poalization [24, 26] with magnetic moment of 3.1 μB. The band gap of $Zn_{30}Sm_1Co_1S_{32}$ is found to be smaller compared to the bulk band gap (3.68 eV) due to band gap undersestimation of DFT. The metallic behaviour at the fermi level in the spin down channel is mainly contributed by Co-3d states hybridized with 3p states of four nearest neighbour S atoms demonstrating a strong p-d hybridization promoting the electron transfer [24–27]. Figure 4 (b) shows the charge density difference contour plot of (Sm, Co) Co-doped ZnS which reveals notable charge accumulation around Co and Sm dopants, with maximum values reaching +0.3 e/Å^3. The contour overlap between the dopants and adjacent S atoms indicates strong hybridization and charge redistribution [28]. This redistribution supports the formation of covalent bonding and the stabilization of the observed ferromagnetic ground state [29]. Such interactions contribute to the observed ferromagnetic ground state by facilitating exchange mechanisms, consistent with the spin-polarized density of states and magnetic moment analysis [30, 31].

4. Conclusion

In summary, first principle calculations are performed in (Sm, Co) Co-doped ZnS DMS using GGA+U approximation. Results show enhanced structural stability with suitable value of formation energy. The Co-doped system shows ferromagnetic behaviour at the higher Sm-Co separation whereas enhanced short range antiferromagnetic interaction dominates for smaller Sm-Co separation. The electronic properties show p-d hybridization between d spins of Co and p spins of S atoms depicting half metallic behaviour with 100% spin polarization. The charge density analysis demonstrates the stabilization of magnetic interactions through hybridization and observed ground state of the system. The results obtained in the present study conclude that (Sm-Co) Co-doped ZnS system is one of the superior rare earth and transition metal Co-doped DMS candidate for spintronics applications.

Authors Contribution
All authors contributed equally to the conception, literature review, and writing of the manuscript. All authors read and approved the final version.

Availability of data and materials
The data that support the findings of this study are available from the corresponding author, upon reasonable request.

Conflict of interests
The authors declare that they have no known competing financial interests or personal relationships that could have appeared to influence the work reported in this paper.

References

[1] W.A. Goddard, D. Brenner, S.E. Lyshevski, and G.J. Iafrate. Hand book of nanoscience, engineering and technology. . (3rd Ed.); CRC press, (2017).

[2] S.A.A. Wolf, Y. Chtchelkanova, and D.M. Treger. Spintronics—A retrospective and perspective. . *IBM J. Res. Dev.*, **50**:101, (2006).

[3] A. Hirohata, K. Yamada, Y. Nakatani Prejbeanu, I. Diény, P. Pirro, and B. Hillebrands. Review on spintronics: Principles and device applications. . *J. Mag. Mag. Mat.*, **509**:166711, (2020).

[4] S.A. Wolf, D.D.R. Awschalom, A.J. Buhrman, M. Daughton, S. Molnár, M.L. Roukes, A.Y. Chtchelkanova, and D.M. Treger.

Spintronics: a spin-based electronics vision for the future. . *Science*, **294**:1488–1495, (2001).

[5] M.I. Miah. Generation and Detection of Spin Current in Semiconductors: Semiconductor Spintronics. . *Mater. Today: Proceed.*, **2**: 5111–5116, (2015).

[6] R. Jansen. Silicon spintronics. *Nature Mater.*, **11**:400–408, (2012).

[7] B. Poornaprakash, S. Sambasivam, D. Amaranatha Reddy, G. Murali, R.P. Vijayalakshmi, and B.K. Reddy. Dopant induced RTFM and enhancement of fluorescence efficiencies in spintronic ZnS:Ni nanoparticles. *Ceram. Int.*, **40**:2677–2684, (2014).

[8] S. Sambasivam, D.P. Joseph, J.G. Lin, and C. Venkateswaran. Doping induced magnetism in Co–ZnS nanoparticles. . *J. Solid State Chem.*, **182**:2598–2601, (2009).

[9] D.A. Reddy, G. Murali, R.P. Vijayalakshmi, and B.K. Reddy. Room-temperature ferromagnetism in EDTA capped Cr-doped ZnS nanoparticles. . *Appl. Phys. A.*, **105**:119–124, (2011).

[10] P. Blaha, K. Schwarz, G.K.H. Madsen, D. Hvasnicka, and J. Luitz. WIEN2k: An Augmented Plane Wave Plus Local Orbitals Program for Calculating Crystal Properties, Vienna University of Technology, Austria. (2001).

[11] B. Kong, T. Zeng, Y.G. Wu, Z.J. Fu, and Z.W. Zhou. Ab initio GGA+U investigations of the electronic properties and magnetic orderings in Mn, Gd doped ZB/WZ structural CdSe. . *Comput. Mater. Sci.*, **142**:14–24, (2018).

[12] A. Twardowski, T. Fries, Y. Shapira, and M. Demianiuk. The d-d exchange interaction in the diluted magnetic semiconductor ZnFeS. . *J. Appl. Phys.*, **73**:6087–6089, (1993).

[13] P. Kaur, S. Kumar, C.L. Chen, K.S. Yang, D.H. Wei, C.L. Dong, C. Srivastava, and S.M. Rao. Gd doping induced weak ferromagnetic ordering in ZnS nanoparticles synthesized by low temperature co-precipitation technique. . *Mater. Chem. Phys.*, **186**:124–130, (2017).

[14] V. Dierolf, I.T. Ferguson, and J.M. Zavada. Rare Earth and Transition Metal Doping of Semiconductor Materials: Synthesis, Magnetic Properties and Room Temperature Spintronics. (2016).

[15] H. Hedjar, S. Meskine, Boukortt A., H. Bennacer, and M.R. Benzidane. First-principles studies of electronic structure, magnetic and optical properties of rare-earth (RE= Sm, Eu, Gd, and Er) doped ZnS. . *Comp. Cond. Mat.*, **30**:e00632, (2021).

[16] H. Hedjar, S. Meskine, A. Boukortt, H. Bennacer, and A. Benaouad. First principles investigations of optoelectronic and magnetic properties of co-doped zinc sulphide by 3d and 4f elements.". *Computational Condensed Matter*, **33**:e00746, (2022).

[17] Z. Liu, X. Wang, and H. Zhu. A new diluted magnetic semiconductor based on the expanded phase of ZnS: surmounting the random distribution of magnetic impurities. *Phys. Chem. Chem. Phys.*, **17**: 13117–13122, (2017).

[18] P. Giannozzi, S. Baroni, N. Bonini, M. Calandra, R. Car, C. Cavazzoni, D. Ceresoli, G.L. Chiarotti, M. Cococcioni, I. Dabo, A. Dal Corso, S. Gironcoli, S. Fabris, G. Fratesi, R. Gebauer, U. Gerstmann, C. Gougoussis, A. Kokalj, M. Lazzeri, L. Martin-Samos, N. Marzari, F. Mauri, R. Mazzarello, S. Paolini, A. Pasquarello, L. Paulatto, C. Sbraccia, S. Scandolo, G. Sclauzero, A.P. Seitsonen, A. Smogunov, P. Umari, and R.M. Wentzcovitch. QUANTUM ESPRESSO: a modular and open-source software project for quantum simulations of materials. . *J. Phys. Condens. Matter.*, **21**:395502, (2009).

[19] J.P. Perdew, K. Burke, and M. Ernzerhof. Generalized Gradient Approximation Made Simple. . Phys. Rev. Lett.:3865, (1996).

[20] H. Yan, Y. Li, Y. Guo, Q. Song, and Y. Chen. Ferromagnetic properties of Cu-doped ZnS: A density functional theory study. . *Physica B.*, **406**:545–547, (2011).

[21] T.H. Fischer and J. Almlof. General methods for geometry and wave function optimization. *J. Phys. Chem.*, **96**:9768, (1992).

[22] A. Jehan, M. Husain, V. Tirth, A. Algahtani, M. Uzair, N. Rahman, A. Khan, and S.N. Khan. Investigation of the structural, electronic, mechanical, and optical properties of $NaXCl_3$ (X = Be, Mg) using density functional theory. *RSC Adv.*, **13**:28395–28406, (2023).

[23] B. Poornaprakash, P.T. Poojitha, U. Chalapathi, K. Subramanyam, and S.H. Park. Synthesis, structural, optical, and magnetic properties of Co doped, Sm doped and Co+Sm co-doped ZnS nanoparticles. *Phys. E Low-dimens. Syst. Nanostruct.*, **83**:180–185, (2016).

[24] Z.H. Yin and J.M. Zhang. Structural, electronic and magnetic properties of the (Co, Ni) codoped ZnS: A first-principles study. *Phys. Lett. A.*, **380**:2796–2802, (2016).

[25] D. Saikia and J.P. Borah. Carrier induced ferromagnetism in half metallic Co doped ZnS diluted magnetic semiconductor. *Appl. Phys. A*, **124**:240, (2018).

[26] M.S. Akhtar, M.A. Malik, S. Raiz, and S. Naseem. Room temperature ferromagnetism and half metallicity in nickel doped ZnS: Experimental and DFT studies. . *Mater. Chem. Phys.*, **160**:440–446, (2015).

[27] D. Saikia, S. Parnamee, and J.P. Borah. Half-Metallic Ferromagnetism in the Co-Doped CdS Diluted Magnetic Semiconductor. *JETP Lett.*, **116**:444–448, (2022).

[28] R. Sonkar, N.J. Mondal, S. Thakur, E. Saikia, M.P. Ghosh, and D. Chowdhury. Cobalt substituted ZnS QDs: a diluted magnetic semiconductor and efficient photocatalysist. . *Nanoscale Adv.*, **5**: 7042–7056, (2023).

[29] M. Shobana and S.R. Meher. Effect of cobalt doping on the structural, optical and magnetic properties of sol-gel derived ZnS nanocrystalline thin films and ab initio studies. . *Thin Sol. Film.*, **683**:97–110, (2019).

[30] H. Hedjar, S. Meskine, A. Boukortt, H. Bennacer, and M.R. Benzidane. First-principles studies of electronic structure, magnetic and optical properties of rare-earth (RE = Sm, Eu, Gd, and Er) doped ZnS. . **30**:e00632, (2022).

[31] H.Q. Xie, L.J. Tang, J.L. Tang, and P. Peng. Magnetic properties of NI-doped ZnS: First-principles study. . *J. Mag. Mag. Mater.*, **377**: 239–242, (2015).